Available online at www.sciencedirect.com
ScienceDirect
Journal of Power Sources 179 (2008) 854–857
JOURNAL OF POWER SOURCES
www.elsevier.com/locate/jpowsour

Short communication

Hydrothermal synthesis of hydrated vanadium oxide nanobelts using poly (ethylene oxide) as a template

Ch.V. Subba Reddy [a], Sun-il Mho [a], Rajamohan R. Kalluru [b,*], Quinton L. Williams [b]

[a] *Division of Energy Systems Research, Ajou University, Suwon 443-749, Republic of Korea*
[b] *Department of Physics, Atmospheric Sciences and Geosciences, 1400, J R Lynch Street, Jackson State University, Jackson, MS 39217-17660, United States*

Received 20 December 2007; received in revised form 4 January 2008; accepted 7 January 2008
Available online 16 January 2008

Abstract

With the aim of obtaining nanodevices as batteries, sensors and fuel cells, we prepared V_2O_5 and $V_3O_7{\cdot}H_2O$ nanobelts by a simple hydrothermal process using poly (ethylene oxide) (PEO) as a template. The yielding percentage of the nanomaterial is less in polymer-free V_2O_5 nanobelts and material size is also big. It is apparent that PEO used $V_3O_7{\cdot}H_2O$ form a continuous and relatively homogeneous matrix with a clearly 1–5 μm long and 50–150 nm diameter nanobelts morphology. The SEM micrographs suggest that there is no bulk deposition of polymer on the surface of the nano-crystallites. Strong interaction between the vanadyl group and the polymer during the formation process has been identified by the shifts of the vanadyl vibration peaks. The CV curve of the electrode made of the $V_3O_7{\cdot}H_2O$ nanobelts have higher current densities than the CV curve of the electrode made of V_2O_5 nanobelts.

Keywords: Vanadium pentoxide xerogel; $V_3O_7{\cdot}H_2O$ nanobelts; Batteries; Fuel cells; Cyclic voltammogram

1. Introduction

Nanoporous materials (nanostructures), which are considered as intermediates between classical molecular scale and micro-sized entities, constitute a rapidly growing field of scientific interest and industrial applications. Well-defined structures of this length scale are difficult to obtain because neither typical physical tailoring techniques nor planned chemical synthesis are especially applicable in this size domain. Since chemical reactivity and physical properties in the nanoregion are strongly dependent on the size of the structures, such materials are very interesting in many respects, particularly for the production of highly functional, finely dispersible, and resource-saving base materials for nanodevices. Nanoparticles may be of quite different shapes such as spheroids, mushrooms [1], platelets, rods, or tubes; the form adopted plays a large role in determining the basic properties, for example, isotropic or anisotropic behavior and region-dependent surface reactivity.

A nanobelt is a nanostructure with rectangular flat tips at the edges. Low dimensional nanostructures of vanadium oxides and their derivatives, including nanoparticles, nanotubes, nanorods, nanobelts, and nanosheets have attracted intensive interest due to their novel physicochemical properties and potential applications in high-energy lithium batteries and chemical sensors. Among them nanobelts with a rectangular cross-section are interesting and expected to represent important building blocks for nanodevices due to higher surface area comparing the nanorods and nanotubes. This higher surface area is useful for large number Li^+ intercalation.

The anisotropic structure of tubular materials, such as the well investigated nanotubes of carbon [2], WS_2 [3], and TiO_2 [3], is linked to interesting physical and chemical properties [4]. At present, such materials are the focus of worldwide investigations because of their outstanding properties that open up visions of various applications as multifunctional nanodevices [5]. Vanadium metal is known to be a catalytically active center in different molecular complexes and inorganic materials. Vanadium peroxo complexes have been used as catalysts and in stoichiometrically conducted reactions as oxo-reagents for alcohols, arenas, alkenes and thioethers [6,7].

* Corresponding author. Tel.: +1 601 979 3613; fax: +1 601 979 3630.
E-mail address: rajamohan.r.kalluru@jsums.edu (R.R. Kalluru).

0378-7753/$ – see front matter © 2008 Elsevier B.V. All rights reserved.
doi:10.1016/j.jpowsour.2008.01.014

Vanadium oxide hydrate ($V_3O_7{\cdot}H_2O$), one of the vanadium oxyhydroxides containing V^{5+} and V^{4+} in a ratio of 2:1, is of interest because of its layered structure and redox activity [7]. Much effort has been expended on the synthesis of low dimensional nanostructured vanadium oxides. Nesper and coworkers used neutral surfactant molecules such as primary aliphatic amines, together with vanadium alkoxide precursors to generate redox-active vanadium oxide nanotubes by hydrothermal method, which is a cost-effective and simple method [8]. Li et al. reported the synthesis of $V_3O_7{\cdot}H_2O$ nanobelts using hydrothermal method from V_2O_5 powder in the presence of hydrochloric acid [9]. Qiao et al. reported the synthesis of $V_3O_7{\cdot}H_2O$ nanobelt cathodes for lithium-ion batteries [10]. Li and coworkers reported the synthesis of nanobelts of metastable vanadium dioxide single-crystal by hydrothermal technique using formic acid as a reducing agent [11]. However, the synthesis of pure $V_3O_7{\cdot}H_2O$ low dimensional nanostructures remains challenging to materials scientists. In this work, the synthesis of V_2O_5 nanobelts and $V_3O_7{\cdot}H_2O$ nanobelts by hydrothermal process from V_2O_5 xerogel, and their application to the electrode materials for electrochemical applications are reported.

2. Experimental

2.1. Synthesis of vanadium oxide nanobelts

The syntheses of template and template-free V_2O_5 nanobelts were performed in three stages. The first step consisted of the preparation of V_2O_5 xerogels [12]. In the second step, 20 ml solution of PEO was added to the 50 ml of V_2O_5 xerogel (molar ratio V_2O_5 xerogel/PEO = 1:0, 0.5 and 1). The resulting light black mixture was stirred for 24 h. Finally, the vanadium oxide and the different composition of vanadium oxide-PEO composite were heated under hydrothermal conditions in a Teflon-lined autoclave at 140 °C for 7 days. The resulting green powder was washed with ethanol and distilled water and then dried under vacuum at 100 °C for about 10 h.

2.2. Characterization

X-ray powder diffraction (XRD) pattern were recorded on HZG4/B-PC diffractometer operating with the Co Kα radiation and graphite monochrometer. Fourier transform infrared (FTIR) absorption spectra of the films were recorded using a 60-SXB IR spectrometer with a resolution of 4 cm^{-1}. The measurements were taken over a wave number range, 400–4000 cm^{-1}. Scanning electron microscope (SEM) recordings were obtained by using a JSM-5610LV microscope. For the DSC measurements a Netzsch STA 409 PC, operating in dynamic mode (heating rate = 10 K min^{-1}), was employed under N_2 gas atmosphere. Samples of ≈5 mg weight were placed in sealed aluminium pans. Prior to use the calorimeter was calibrated with metal standards; an empty aluminium pan being used as a reference. The electrochemical properties of the V_2O_5 and $V_3O_7{\cdot}H_2O$ nanobelts were investigated by using a three-electrode cell with a platinum counter electrode and a silver wire in the 0.1 mol l^{-1} AgCl solution as the reference electrode. The working electrode, prepared by mixing 75 wt% of active material, 20 wt% of carbon black and 5 wt% of ethylene cellulose, was then coated on a 1.5-cm^2 ITO glass. A 1-mol l^{-1} solution of lithium perchlorate (99.99%, Aldrich) in propylene carbonate (99.7%, Aldrich) was used as the electrolyte. Cyclic voltammetric (CV) measurements were carried out between the potential limits of −1.0 and 1.0 V against Ag/AgCl using a potentiostat/galvanostat (Zahner IM6). The CV curves were recorded at a scan rate of 10 mV s^{-1}.

3. Results and discussion

Scanning electron micrographs of template-free V_2O_5 nanobelts and template used $V_3O_7{\cdot}H_2O$ nanobelts are shown in Fig. 1. The yielding percentage of the nanobelts is less in template-free V_2O_5 nanomaterial and material size is also bigger. It is apparent that $V_3O_7{\cdot}H_2O$ forms a continuous and relatively homogeneous matrix with a clearly 1–5 μm long and 50–150 nm diameter nanobelts morphology. It is evident that the incorporation of PEO into the lattice during the $V_3O_7{\cdot}H_2O$ nanobelts formation process leads to morphological changes.

Fig. 2 shows the XRD patterns of the V_2O_5 nanobelts and vanadium oxide hydrate ($V_3O_7{\cdot}H_2O$) nanobelts prepared by the hydrothermal processes with template-free and with template (PEO) used, respectively. The strongest peak observed at the low angle corresponds to the (0 0 1) plane of the layered V_2O_5 structure in vanadium oxide nanobelts. All remaining diffraction peaks can be indexed to the orthorhombic system with the lattice constants a = 11.516 Å, b = 3.5656 Å and c = 4.37275 Å (JCPDS #41–1426) [13–14]. All diffraction peaks of the vanadium oxide hydrate ($V_3O_7{\cdot}H_2O$) can be indexed to the orthorhombic system with the lattice constants a = 9.34 Å, b = 17.0 Å and c = 3.626 Å (JCPDS 28-1433). No peaks related to polymers were observed in the XRD pattern of vanadium oxide hydrate ($V_3O_7{\cdot}H_2O$) nanobelts. Vanadium oxides with mixed valency, containing V^{5+} as well as V^{4+} cations, were usually obtained by hydrothermal processing of precursor and reductive organic molecules [15]. In the present study, during the hydrothermal synthetic process from the V_2O_5 xerogel, the polymer PEO served as a template as well as a reducing agent. The products were in green colour after the hydrothermal process, which indicates V^{5+} cations partially reduced to V^{4+} cations. The PEO played a critical role in the formation of $V_3O_7{\cdot}H_2O$ nanobelts during the hydrothermal process. Polymers such as PVP, PEO, and PEG are multidentate ligands with poly functional groups, which can serve as bridging ligands to form multinuclear complexes [16]. We assumed that a coordination complex PEO_x-$V_3O_7{\cdot}H_2O$ was formed during the hydrothermal processes, based on the phase diagram of V (V) in aqueous solutions [8]. The PEO molecule chain may afford its O atoms to coordinate with the polyvanadate ions.

The IR spectra of template-free V_2O_5 nanobelts and template used $V_3O_7{\cdot}H_2O$ nanobelts are shown in Fig. 3. A broad band at 3472 cm^{-1} corresponding to the O–H vibration confirms [12] the presence of water in the V_2O_5 xerogel before use of the template. The V_2O_5 nanobelts exhibit three main vibration modes in the 500–1040 cm^{-1} region. The terminal oxygen symmetric stretching mode (ν_s) of V=O and the bridge oxygen asymmetric and symmetric stretching modes (ν_{as} and ν_s) of

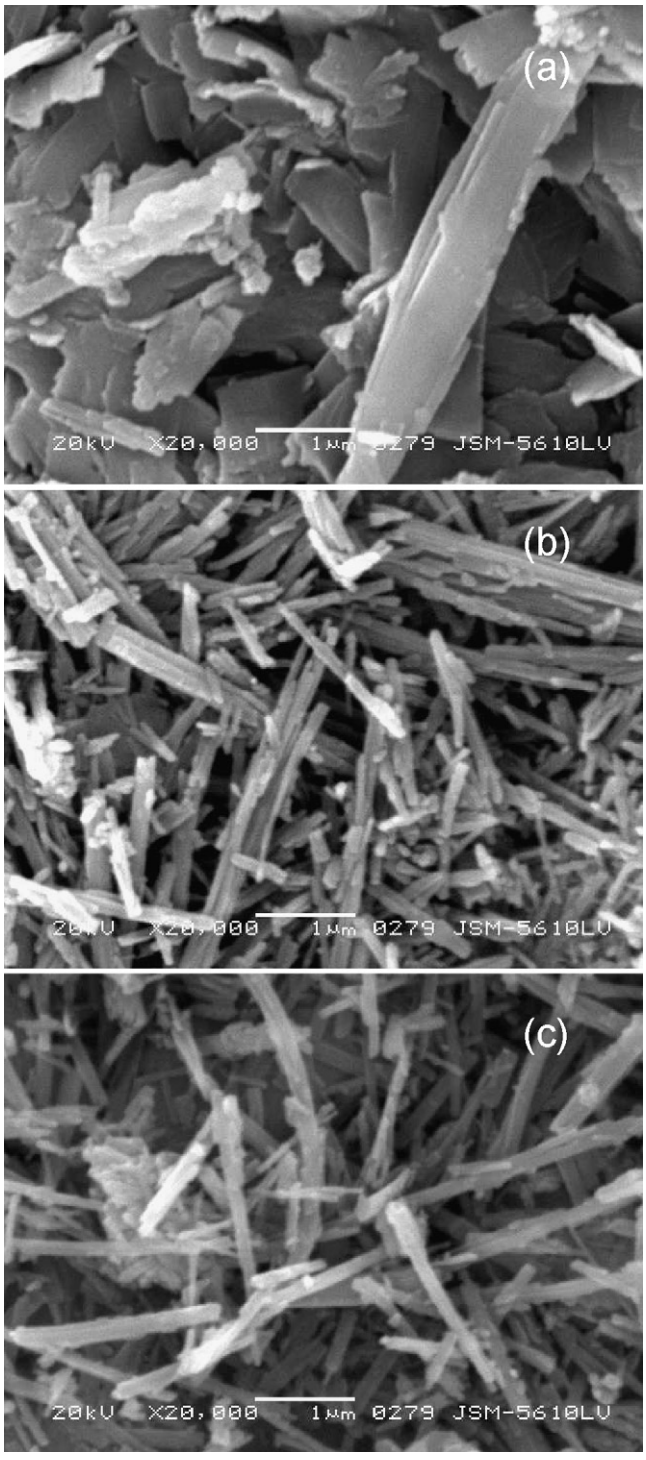

Fig. 1. SEM micrographs of nanobelts of (a) template-free V_2O_5, (b) 0.5 M template used $V_3O_7{\cdot}H_2O$, and (c) 1 M template used $V_3O_7{\cdot}H_2O$.

V–O–V are at 1022, 850 and 524 cm^{-1}, respectively [12]. The ν_s (V–O–V) and ν_{as} (V–O–V) modes shift to longer wave numbers. The ν_{as} (V–O–V) mode shifts from 850 cm^{-1} to 970 cm^{-1}. The ν_s (V–O–V) mode moves from 524 cm^{-1} to 570 cm^{-1} and the ν_s (V=O) band shifts from 1022 cm^{-1} to 1029 cm^{-1} [17]. The shifts in the vibration modes (ν_{as} and ν_s) indicate the reduction of the vanadium oxidation state.

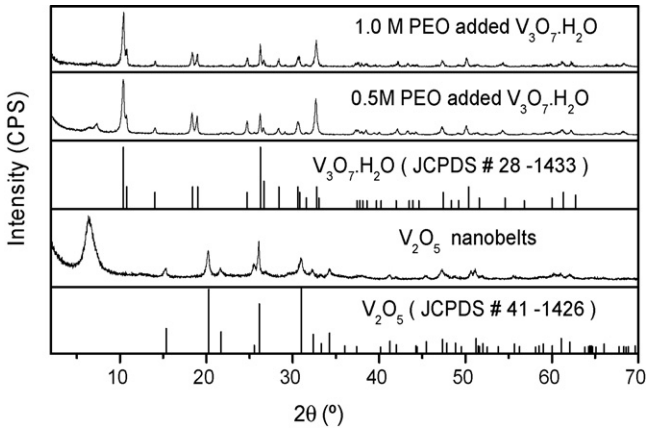

Fig. 2. XRD patterns of the vanadium oxide (V_2O_5) and vanadium oxide hydrate ($V_3O_7{\cdot}H_2O$) nanobelts.

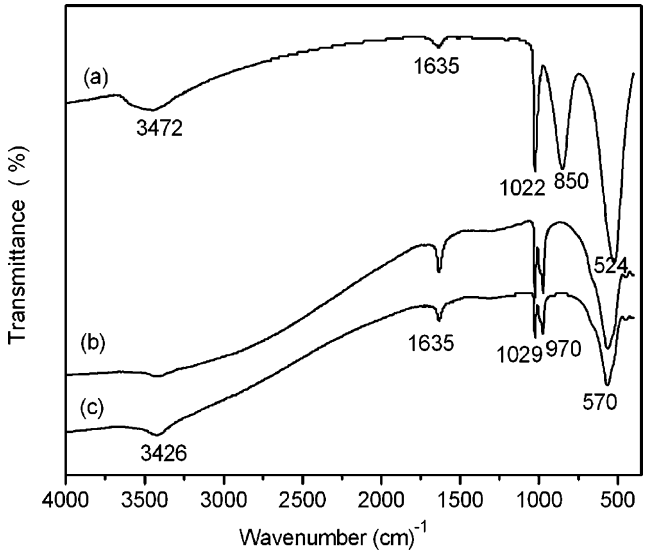

Fig. 3. IR spectra of nanobelts of (a) template-free V_2O_5, (b) 0.5 M template used $V_3O_7{\cdot}H_2O$, and (c) 1 M template used $V_3O_7{\cdot}H_2O$.

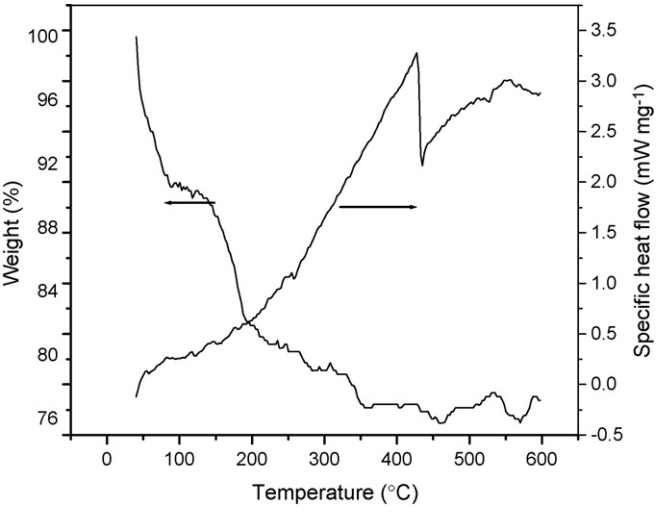

Fig. 4. TG-DSC curves of 0.5 M template used $V_3O_7{\cdot}H_2O$ nanobelts.

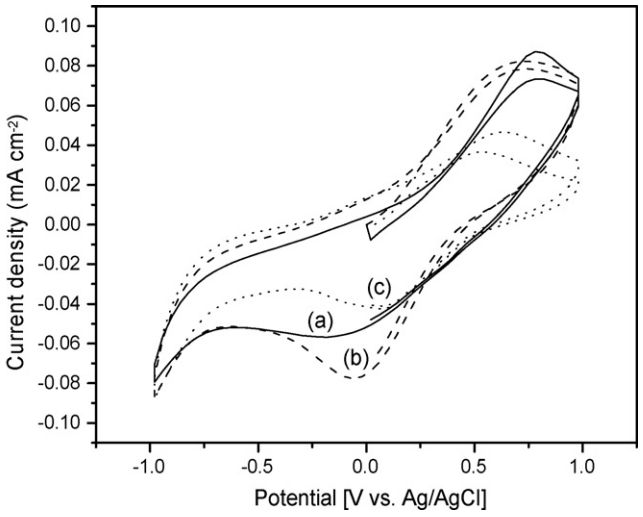

Fig. 5. Cyclic voltammograms of nanobelts of (a) template-free V_2O_5, (b) 0.5 M template used $V_3O_7{\cdot}H_2O$, and (c) 1 M template used $V_3O_7{\cdot}H_2O$ obtained with scan rate 10 mV s^{-1} in a 1 M $LiClO_4$ dissolved in propylene carbonate electrolyte.

Fig. 4 shows the thermogravimetry (TG) and differential scanning calorimetry (DSC) curves of the template used $V_3O_7{\cdot}H_2O$ nanobelts. The TG curves can be divided into three temperature domains of 40–90, 90–270 and 270–460 °C. The first step up to 90 °C is attributed to removal of water. Next weight loss until 190 °C is due to the combustion of the polymer component. The abrupt weight loss around 150 °C is assigned to the decomposition of the ethylene oxide groups of the polymer. A mass gain to 460 °C is ascribed to the exothermic oxygen uptake, which occurs together with the conversion of V^{4+} into V^{5+} [18].

Cyclic voltammograms of template-free V_2O_5 nanobelts and template used $V_3O_7{\cdot}H_2O$ nanobelts are shown in Fig. 5. The cyclic voltammograms of the template-free V_2O_5 nanobelts show broad cathodic reduction peak at −0.07 V, which corresponds to Li^+ intercalation (electrical energy is stored in the form of a chemical potential) and anodic oxidation peak at 0.77 V, which is attributed to Li^+ extraction (chemical energy is released in the form of electricity). The cyclic voltammograms of the template used $V_3O_7{\cdot}H_2O$ nanobelts also show cathodic peak at −0.05 V (Fig. 5b) and 0.07 V (Fig. 5c), and anodic peak at 0.64 V (Fig. 5b), and 0.65 V (Fig. 5c). The CV curve of the electrode made of the $V_3O_7{\cdot}H_2O$ nanobelts have higher current densities than the CV curve of the electrode made of V_2O_5 nanobelts.

4. Conclusions

Template-free V_2O_5 nanobelts and template used $V_3O_7{\cdot}H_2O$ nanobelts have been synthesized and subjected to various characterizations. Thermal characteristics of template used $V_3O_7{\cdot}H_2O$ nanobelts were assessed by thermal analysis method. The decomposition route was found to be a three-step process. The cyclic voltammogram measurements show that template used $V_3O_7{\cdot}H_2O$ nanobelts have higher Li^+ ions intercalation than the template-free V_2O_5 nanobelts.

Acknowledgement

This research was in part supported by the Korea Science and Engineering Foundation (KOSEF R01-2007-000-20223-0).

References

[1] S.I. Stupp, V. LeBonheur, K. Walker, L.S. Li, K.E. Huggins, M. Keser, A. Amstutz, Science 276 (1997) 384.
[2] P.M. Ajayan, Chem. Rev. 99 (1999) 1787.
[3] R. Tenne, M. Homyonfer, Y. Feldman, Chem. Mater. 10 (1998) 3225.
[4] T. Kasuga, M. Hiramatsu, A. Hoson, T. Sekino, K. Niihara, Langmuir 14 (1998) 3160.
[5] C.N.R. Rao, B.C.S. Kumar, A. Govindaraj, M. Nath, Chem. Phys. Chem. 2 (2001) 78.
[6] V. Conte, F. Di Furia, G. Licini, Appl. Catal. A 157 (1997) 335.
[7] Y. Oka, T. Yao, N. Yamamoto, J. Solid State Chem. 89 (1990) 372.
[8] M.E. Spahr, P. Bitterli, R. Nesper, M. Müller, F. Krumeich, H.U. Nissen, Angew. Chem. Int. Ed. 37 (1998) 1263.
[9] G.C. Li, S.P. Pang, Z.B. Wang, H.R. Peng, Z.K. Zhang, Eur. J. Inorg. Chem. 11 (2005) 2060.
[10] H. Qiao, X. Zhu, Z. Zheng, L. Liu, L. Zhang, Electrochem. Commun. 8 (2006) 21.
[11] J. Liu, Q. Li, T. Wang, D. Yu, Y. Li, Angew. Chem. Int. Ed. Engl. 43 (2004) 5048.
[12] C.V. Subba Reddy, X. Han, A.-P. Jin, Q.-Y. Zhu, L.-Q. Mai, W. Chen, Electrochem. Commun. 8 (2006) 279.
[13] P. Balog, D. Orosel, Z. Cancarevic, C. Schön, M. Jansen, J. Alloys Compd. 429 (2007) 87.
[14] A.V. Murugan, M.V. Reddy, G. Campet, K. Vijayamohanan, J. Electroanal. Chem. 603 (2007) 287.
[15] J. Livage, Coord. Chem. Rev. 178 (1998) 999.
[16] Y. Deng, G.D. Wei, C.W. Nan, Chem. Phys. Lett. 368 (2003) 639.
[17] S. Shi, M. Cao, X. He, H. Xie, Cryst. Growth Des. 7 (2007) 1893.
[18] F. Sediri, F. Touati, N. Gharbi, Mater. Sci. Eng. B 129 (2006) 251.